

# SIMULATION STUDY ON THE FORMATION OF PLGA MICRO-STRUCTURE USING HOT-PRESSING METHOD

Gao, Y.<sup>\*,#</sup>; Xu, C.<sup>\*</sup>; Yang, L.<sup>\*</sup> & Wang, B.<sup>\*\*</sup>

<sup>\*</sup> School of Mechanical Engineering, Xi'an University of Science and Technology, Xi'an, 710054, China

<sup>\*\*</sup> School of Mechanical Engineering, Brunel University London, Uxbridge, London, UB8 3PH, UK  
E-Mail: gaoyangyang@xust.edu.cn (# Corresponding author)

## Abstract

A novel controlled drug delivery system was proposed, which contains a micro-structure for drug loading fabricated by using Poly(lactic-co-glycolic acid) (PLGA) via the hot-pressing method. The integrity of the PLGA micro-structure is the basis of the drug release control, but the visco-elastic property of PLGA causes the incomplete formation in the hot-pressing process. To obtain the improved hot-pressing parameters, the hot-pressing model of PLGA materials was established by using a 5-unit generalized Maxwell model. The influence of different hot-pressing parameters on the forming quality was studied. Simulation results show that the PLGA micro-structure was completely formed at the temperature of 75 °C, 1 mm base thickness, 30 N pressure, and 150 s maintenance time. The simulation results were validated by the hot-pressing fabrication. This study could lead theoretical basis for the preparation of visco-elastic polymer micro-structure by using the hot-pressing method and lay a foundation for the further optimization of hot-pressing process parameters.

(Received in August 2019, accepted in November 2019. This paper was with the authors 1 month for 1 revision.)

**Key Words:** Visco-Elastic Property, PLGA Micro-Structure, Hot-Pressing Method, Process Parameters

## 1. INTRODUCTION

Biomaterials continue to play a critical role in the successful design of medical devices, especially in controlled drug delivery systems (CDDS) [1]. CDDSs produced by using biomaterials is an important research area due to several outstanding properties, such as long release cycle, high targeting ability, and stable drug release concentrations. CDDSs exhibit broad potential applications to fit the clinical demands for targeted drug release with stable drug concentrations in long-term treatments. Examples of such treatments include adjuvant therapy after surgery, relief of post-operative pain and long-term treatments for chronic diseases. CDDSs with different structures and application purposes have already been reported. Examples contain the nano-fibrous for cancer treatment [2], budesonide-cyclodextrin complex-loaded micro-particles for intranasal application [3], hollow polymeric nano-capsules [4], needle-sized bio-cage for direct local delivery of agents [5].

In this study, a novel CDDS was proposed. It consists of the depot-composed degradable drug carrier, drugs, and the bonding membrane. The maximum dimension of this CDDS is 10 mm in diameter. The drug-depot depth is 400–500 μm. A schematic diagram of this novel CDDS material is shown in Fig. 1. This CDDS featured micro-structure arrays for drug storage and micron-scale holes in its bonding membrane. Moreover, it achieved a nearly stable cumulative release rate [6].

Using heat to form the materials is the main basis principle, not only metallic material [7-9] but also non-metallic material. Through a combination of biomedical techniques and micro-electro-mechanical systems (MEMS), a variety of methods can be used for the formation of polymer micro-structures. Examples for such processes include hot-pressing [10], injection moulding [11, 12] and 3D printing [13, 14].

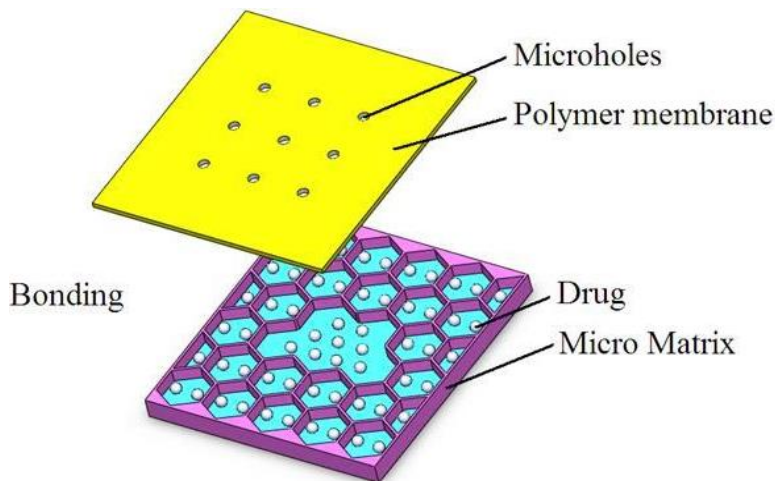


Figure 1: Schematic of the biodegradable CDDS.

In this study, the hot-pressing method was chosen to fabricate the polymer micro-structure of the CDDS for the lower cost and simple operability. In the hot-pressing process, the polymer does not need to be transported over long distances into the moulding tool, thereby reducing shrinkage during the cool down process and further reducing friction forces in the micro-structure during mould unloading. Thus, the delicate micro-structures with higher aspect ratios can be fabricated using the hot-pressing method. Many research groups around the globe have studied polymer formation by the hot-pressing method. The poly(dimethyl siloxane) (PSMS) micro-structure was high fidelity formed using the thermal imprint method [15]. Kiew et al. [16] studied the Poly(Methyl Methacrylate) (PMMA) pattern formation during hot embossing process by the finite element analysis. The pressure distribution of polymer materials in hot-pressing was simulated by Hung et al. [17]. The deformation of PMMA was studied with time and resist thickness evolution [18]. The low temperature thermal nanoimprint lithography using a viscoelastic model was studied by Kim et al. [19]. Lan et al. studied the relaxation features of PC polymer at the glass transition temperature [20].

The above experimental and simulation studies on polymer hot-pressing formation mostly focused on the PMMA or PC. The polymer used in this study is Poly(lactic-co-glycolic acid) (PLGA) with the glass transition temperature at 45-50 °C. PLGA materials are commonly used in CDDS, but the deformation characteristic in a micro-structure formed by the hot-pressing has not yet been studied. The integrality of the CDDS is critical for achieving satisfactory drug release properties. An incomplete drug carrier causes the strength reduction and drug leakage, thereby ultimately inhibiting the overall control of the release rate. Since a polymer usually exhibits macromolecular chains, the material possesses the stress relaxation and visco-elastic properties in the hot-pressing process. Furthermore, the deformation properties are time-dependent due to the specific entropy elasticity of polymer chains. Therefore, the reasonable hot-pressing parameters to get the micro-structure complete formation need to be studied.

The aim of this study was to investigate the suitable hot-pressing parameters of PLGA micro-structure. Firstly, the numerical visco-elastic model of degradable material was established based on a generalized Maxwell model with five units. Secondly, based on the formation model, the PLGA material filling processes were simulated by the finite element method at different formation temperatures, pressures, action times, and substrate thicknesses. Finally, the formation experiments were conducted to verify the rationality of the numerical material model and the simulation results.

## 2. MODEL AND METHOD

### 2.1 Visco-elastic model of PLGA

For the entropy elasticity of polymeric macromolecular chains, the mechanical behaviour of polymers above the glass transition temperature is dependent on the temperature and time. In this case, a temperature-dependent linear elastic-model [21] and a nonlinear elastic model such as the Moony-Rivlin model [22] were not suitable for PLGA formation. Therefore, a generalized Maxwell model was used to describe the modelling behaviour of the visco-elastic materials in the hot-pressing process, in which springs and dampers simulate the linear elastic response and the linear viscous response, respectively. Due to the assumption that the macromolecular chains in PLGA are entangled, the ultimate relaxation modulus of PLGA is not zero as it would be for a linear polymer. In this situation, an extra spring,  $G_\infty$ , must be introduced and paralleled on the generalized Maxwell model. The schematic of the PLGA deformation model is shown in Fig. 2.

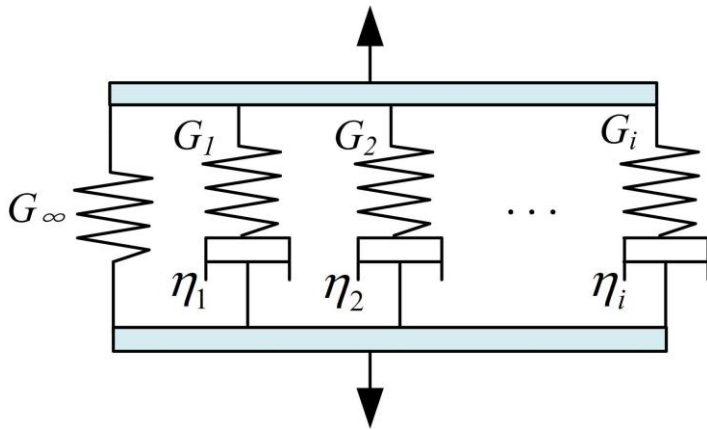


Figure 2: Schematic of the PLGA visco-elastic property.

The time-dependent relaxation modulus ( $G(t)$ ) can be described by a mechanical model with a sufficient number of elastic and viscous elements, it is expressed as an exponential series as follows:

$$G(t) = G_\infty + \sum_{i=1}^n G_i \exp\left(-\frac{t}{\tau_i}\right) \quad (1)$$

$$G_0 = G(t=0) = G_\infty + \sum_{i=1}^n G_i \quad (2)$$

where  $G(t)$  is the relaxation modulus,  $n$  is the number of damp-spring units,  $G_\infty$  is the relaxation modulus of limitation, and  $\tau_i$  is the relaxation time.

### 2.2 PLGA hot-pressing model

The 75/25 PLGA material was used to form the CDDS, and  $30 \times 5 \times 1.5$  mm PLGA test samples were fabricated in advance to obtain the PLGA materials parameters. A dynamic mechanical analyser (DMA-Q800) was used to conduct the materials relaxation experiments. According to the Williams–Landel–Ferry (WLF) equation and the results of the relaxation experiments, the parameters of the generalized Maxwell model with five units are listed in Table I.

Table I: Parameters of generalized Maxwell model [23].

Parameters	Value	Parameters	Value
$G_\infty$	0.00017	--	--
$G_1$	0.16845	$\tau_1$	1.21
$G_2$	0.3181	$\tau_2$	19.73
$G_3$	0.31483	$\tau_3$	113.27
$G_4$	0.17621	$\tau_4$	396.38
$G_5$	0.05149	$\tau_5$	1565.40

The finite element method is widely used in engineering study [24]. In this study, ANSYS was used to model and simulate the deformation behaviour of the PLGA substrate to form a micro-structure via the hot-pressing process. Fig. 3 is the geometry model. For the symmetry shape of the micro-structure, half of the groove template was used as the analysis object. The deepness of the template ( $H$ ) was 540  $\mu\text{m}$ , the half of width ( $L/2$ ) was 60  $\mu\text{m}$ , and the half of spacing ( $S/2$ ) was 800  $\mu\text{m}$ .

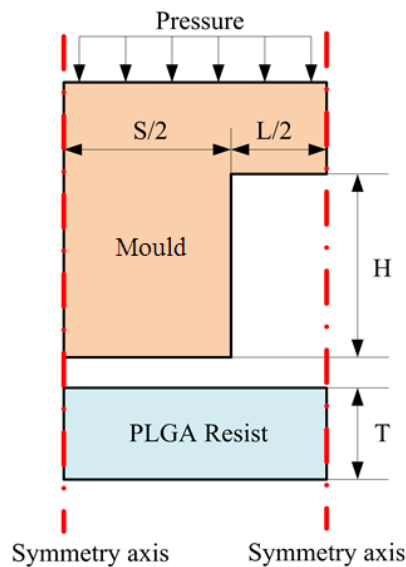


Figure 3: Geometry model of micro-structure formation.

In the analysis, it was assumed that no relative slip existed in the contact surface of the template and the PLGA substrate. Boundary conditions on the left and right boundaries were symmetrical, the bottom of the PLGA membrane was limited, and a constant pressure was applied to the perpendicular template surface. The temperature distribution in this model was even. The template material was PDMS, which has an elastic modulus of 3 MPa and a Poisson's ratio of 0.499.

### **3. RESULTS AND DISCUSSION**

To obtain the information on the quantifying influences of the process parameters that determine the micro-structure formation, factors including pressure, time, temperature, initial substrate thickness, and the aspect ratio of the template were studied using the above mentioned formation model.

#### **3.1 Influence of the pressure and acting time**

The PLGA substrate filling the template groove under the acting pressure and deformation degree was related to the time of pressure action. Therefore, the influences of time-pressure

on the micro-structure formation were studied. Fig. 4 shows the same template groove filled by PLGA at 80 °C and under pressures of 20, 30, and 40 N. The corresponding pressure action times were 20, 50, and 70 s. Fig. 5 shows the filling rates versus time with different pressures and action times.

As shown in Fig. 4, higher formation pressure and longer action time had a tendency to result in better micro-structure quality. For every increase in formation pressure, the height of the filled polymer in the groove template was increased with elapsing action time. The filling speed was directly proportional to the higher pressure. The filling rate is defined as the area ratio of the template groove and the filled PLGA. The 100 % filling rate represents the complete formation of the micro-structure.

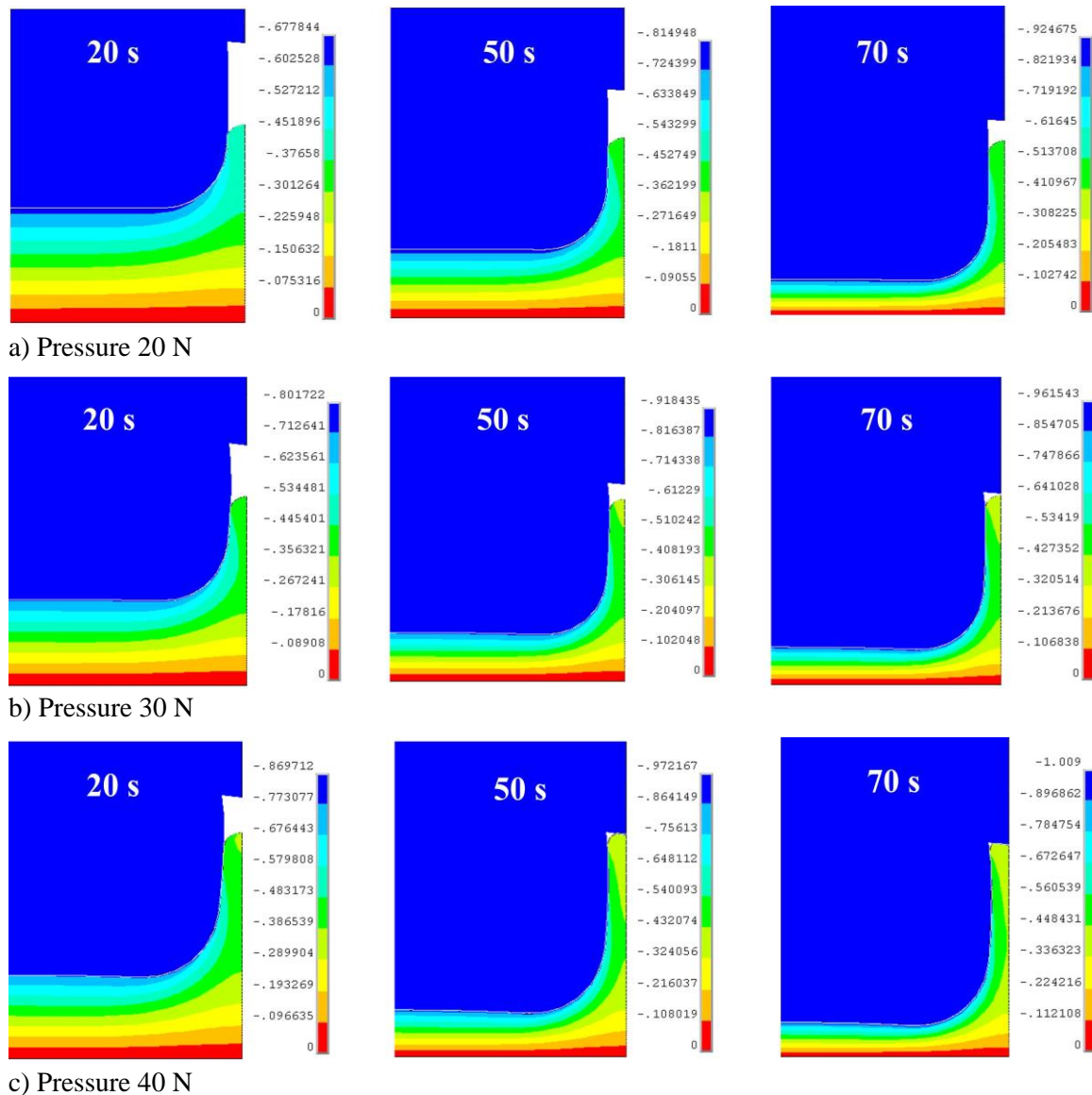


Figure 4: Filling process of PLGA at 80 °C at different pressures and maintenance times.

As shown in Fig. 5, the polymer filling rate increased with increasing corresponding action time of every pressure level. In contrast, for the filling rate with different pressures at the same action time, the higher pressure lead to the high filling rate and short formation time. 200 s is required to completely fill the mould with the pressure of 20 N for the PLGA. As the pressure increased to 40 N, the filling rate was nearly 100 % within a time frame of only about 50 s.

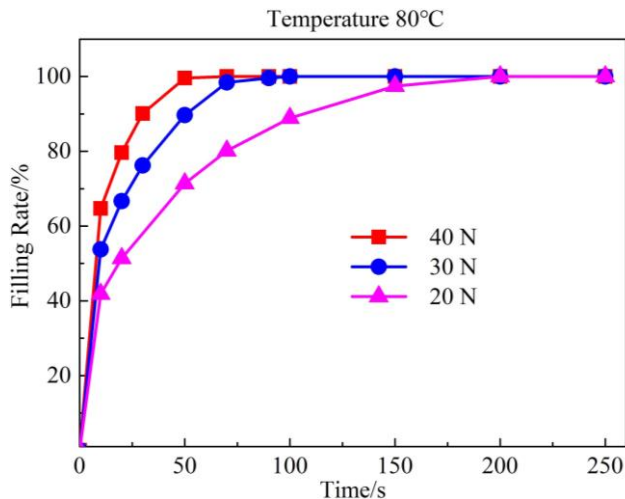


Figure 5: Filling rate with different pressures and acting time at 80 °C.

For the visco-elastic properties of the PLGA, the changes of the filling rate were not in linear relationship with the pressure action time. The chains of the PLGA macromolecular were entangled. Thus, a certain time period was required for the deformation of the PLGA upon applying pressure. A longer action time resulted in the complete release of the internal stress, thereby resulting in the easier deformation and improved formation quality. However, higher pressure, such as 40 N, can accelerated the movement of macromolecular chains, ultimately resulting in an easier filling process.

### 3.2 Influences of moulding temperature

Temperature is another critical factor in the behaviour of the visco-elastic polymers in the hot-pressing process. Temperature directly affects the relaxation properties of the macromolecular PLGA. Fig. 6 highlights the filling process of the same template groove at 70 °C, 75 °C, and 80 °C, respectively, with an applied pressure of 30 N and an action time of 100 s. The formation quality of the micro-structure wall improved with increasing the temperature. Fig. 7 shows the filling rates at different temperatures.

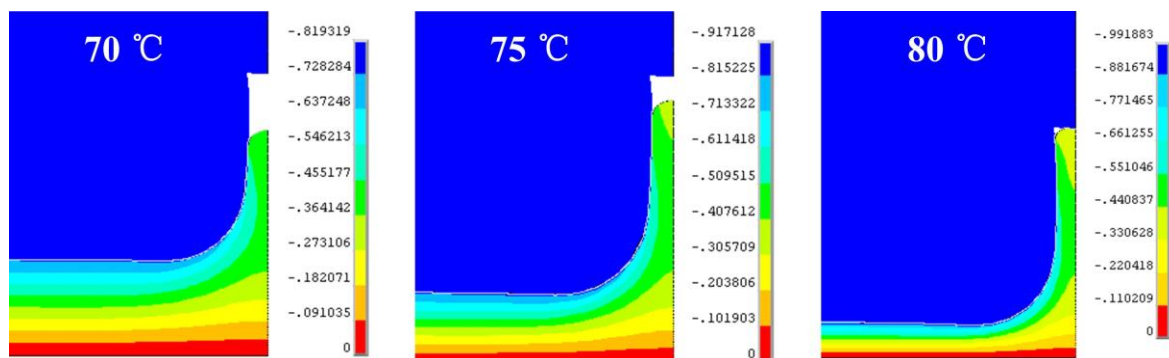


Figure 6: Filling process of PLGA at different temperatures.

According to Fig. 7, to get the 100 % filling rate, 350 seconds is required at 70 °C, whereas only 100 seconds is required at 80 °C. This phenomenon was impossible due to the large elastic modulus of the PLGA. The entangled macromolecular chains of the PLGA need time to relax, and the higher temperature, such as 80 °C, can accelerate the chains relax process. On the other hand, to achieve an improved micro-structure quality at a lower formation temperature such as nearby the PLGA glass-transition temperature 50-55 °C, the maintenance time or the applied embossing pressure is required to be increased.

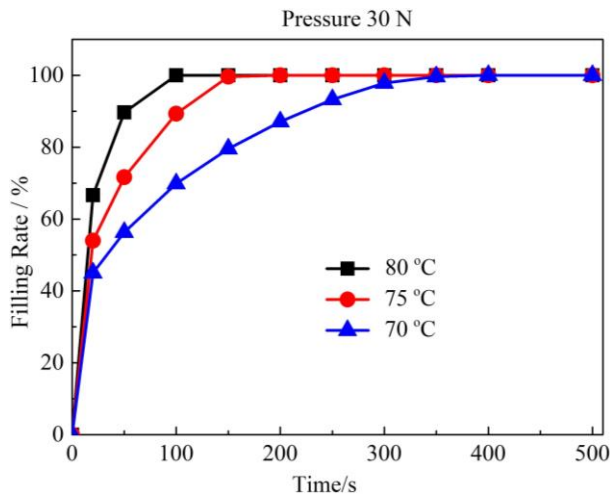


Figure 7: Filling rates at different formation temperatures.

### 3.3 Influence of polymer initial thickness

Insufficient PLGA substrate thickness will not support a sufficient amount of materials for the formation of a micro-structure. However, an exceedingly large thickness of the PLGA substrate has a negative impact on the drug release characteristics, because the release mechanism of CDDS was directly related to the matrix degradation. Therefore, the third parameter affects the micro-structure formation which was the initial thickness of the substrate.

In Fig. 8, Y axis is the pressure to achieve a 100 % filling rate of the template groove, and X axis is the ratio of the initial thickness of the PLGA substrate ( $T$ ) and the height of the template groove ( $H$ ). The formation temperatures were 75 °C and 80 °C.

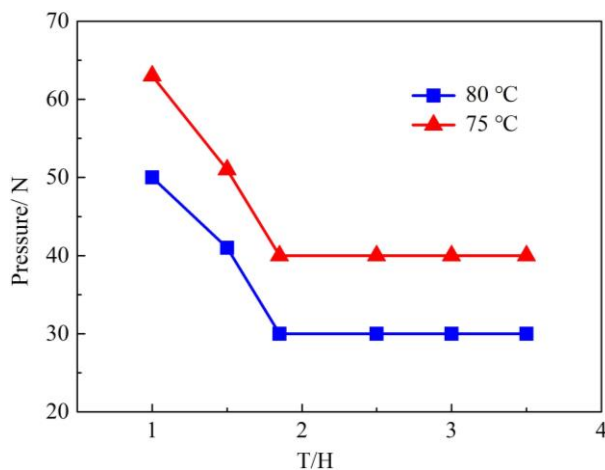


Figure 8: Pressure required for 100 % filling rate at different values of  $T/H$  and temperatures.

The curves in Fig. 8 exhibited an identical change behavior as the value of  $T/H$  growing. When the value of  $T/H$  is less than 1.85, the pressure appeared to be directly proportional to the value of  $T/H$ , whereas the pressure maintains as a constant when the value of  $T/H$  is greater than 1.85. Greater pressure was required to ensure that the PLGA fills the mould completely. An adequate thickness of the PLGA substrate ensures enough materials to fill the micro-structure mould, thereby maintaining the required pressure for the 100 % filling rate.

Based on the above analysis, increasing the substrate thickness will effectively reduce the required formation pressure and improve the formation quality. However, when the value of  $T/H$  is greater than 1.85, enough material can be squeezed into the mould groove, thereby

further increasing the thickness of the substrate has little influence on the moulding pressure but could cause a waste of material. Therefore, in the hot-pressing process, the initial substrate thickness should be controlled around 1.85 times the mould groove depth.

### 3.4 Influence of groove aspect ratio

The high aspect ratio micro-structure is difficult to be fabricated in the hot-pressing process due to the possible incomplete modelling of the structure. Micro-structure integrity plays a critical role in the drug delivery. Thus, the simulation was conducted with a fixed depth of the template groove ( $H$ ) at 540  $\mu\text{m}$  and at the varying width ( $L$ ). The formation temperatures were 75  $^{\circ}\text{C}$  and 80  $^{\circ}\text{C}$ . The changing pressure requirements of the 100 % filling rate and versus the ratio of  $H/L$  are shown in Fig. 9.

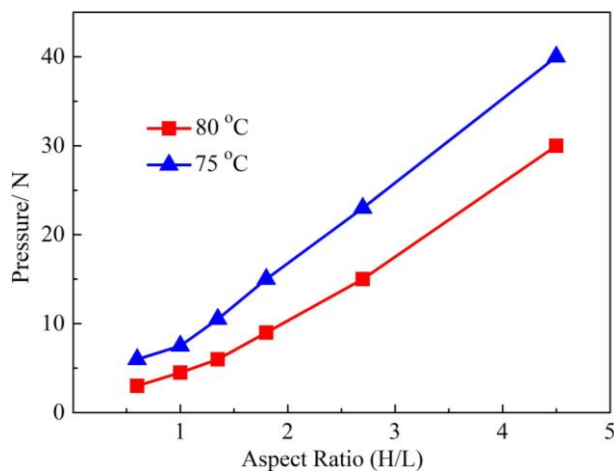


Figure 9: Pressure required for 100% filling rate versus aspect ratio.

As shown in Fig. 9, the pressure required for a filling rate of 100 % indicated a linear relationship to the ratio  $H/L$  at a formation temperature of 80  $^{\circ}\text{C}$  and an applied pressure of 45 N. The entangled macromolecular chains required a large amount of pressure to be squeezed into the groove, so at 75  $^{\circ}\text{C}$ , the required pressure is 7.5 N to get the 100 % filling rate when the  $H/L$  is 1, whereas the required pressure is 40 N to get the 100 % filling rate when the  $H/L$  is 4.5. The filled PLGA with  $H/L$  values of 1 and 4.5 with the same other formation parameters are shown in Fig. 10.

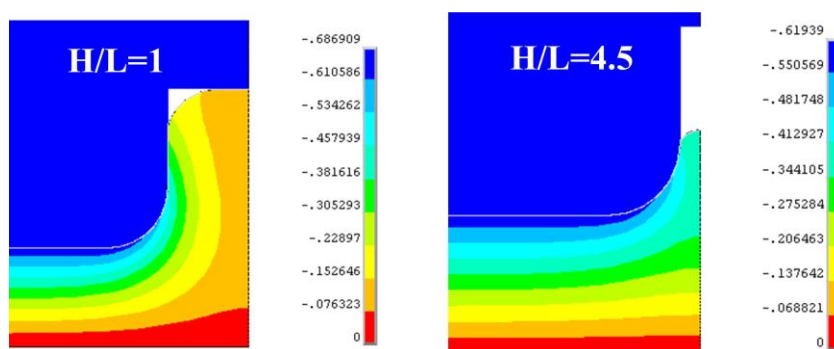


Figure 10: Filled PLGA in mould with different aspect ratios.

### 3.5 Formation experiments

To verify the validity of simulation results, a series of experiments were carried out based on the simulation studies. With the 100 % filling rate as the target, the corresponding parameters of pressure and temperature in experiments are listed in Table II.



Table II: Time-required for 100 % filling rate at different temperatures and pressures.

Pressure (N)	20			30			40		
Temperature (°C)	70	75	80	70	75	80	70	75	80
Time (s)	750	300	190	380	150	100	250	100	65

As shown in Table II, the formation time shortened with increasing temperature and the pressure from 750 s to 65 s. At 80 °C and 40 N, PLGA was easily to fill the micro-structure mould for the fine flow performance; the required time to complete formation is only 65 s, whereas the fine flow performance of PLGA leads the thickness of the residual layer too thin to work efficiently as a drug carrier system. Therefore, based on the simulation analysis, experiments and practical requirements, the suitable formation parameters for a 75/25 PLGA micro-structure were 75 °C, 30 N, and 150 s. The thickness of the initial substrate was 1 mm. The hot-pressing process was carried out with the above parameters, and the corresponding results are shown in Fig. 11. The formed micro-structure exhibited a completely symmetrical structure, and the overall quality was closely as expected.

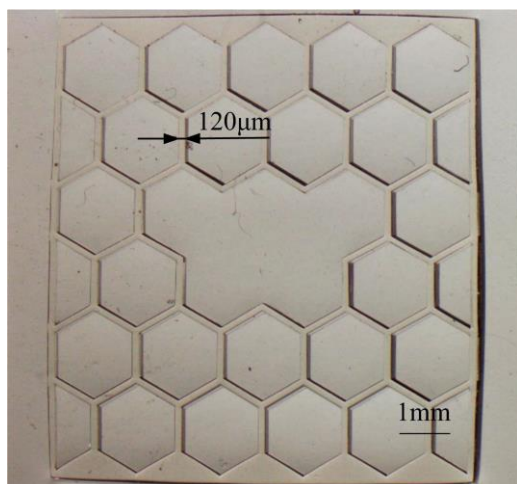


Figure 11: The PLGA micro-structure samples.

#### **4. CONCLUSION**

A hot-pressed model of the PLGA micro-structure was established. The hot pressing process was simulated with the different parameters. The simulation results were verified by the experiments. The conclusions are as follows:

(1) For the entropy elasticity of polymeric macromolecular chains, the mechanical behaviour of polymers above the glass transition temperature was dependent on temperature and time. This visco-elastic character of the PLGA can be reasonably simulated by the damp-spring system and the 5-unit generalized Maxwell model.

(2) The influence of different parameters on the forming quality was studied. The simulation results show that the initial substrate thickness should be controlled around 1.85 times the mould groove depth. The polymer micro-structure was complete formed with at temperature 75 °C, 1 mm base thickness, 30 N pressure, and 150 s maintenance time.

#### **ACKNOWLEDGEMENT**

The authors gratefully acknowledge the support of the National Natural Science Foundation of China (No. 51605379), Basic Research Plan of Natural Science of Shaanxi Province (2019JQ-804).

**REFERENCES**

- [1] Zhang, H.; Jackson, J. K.; Chiao, M. (2017). Microfabricated drug delivery devices: design, fabrication, and applications, *Advanced Functional Materials*, Vol. 27, No. 45, paper 1703606, doi:[10.1002/adfm.201703606](https://doi.org/10.1002/adfm.201703606)
- [2] Xie, M.; Fan, D.; Chen, Y.; Zhao, Z.; He, X.; Li, G.; Chen, A.; Wu, X.; Li, J.; Li, Z.; Hunt, J. A.; Li, Y.; Lan, P. (2016). An implantable and controlled drug-release silk fibroin nanofibrous matrix to advance the treatment of solid tumour cancers, *Biomaterials*, Vol. 103, 33-43, doi:[10.1016/j.biomaterials.2016.06.049](https://doi.org/10.1016/j.biomaterials.2016.06.049)
- [3] Kim, J.-E.; Cho, H.-J.; Kim, D.-D. (2014). Budesonide/cyclodextrin complex-loaded lyophilized microparticles for intranasal application, *Drug Development and Industrial Pharmacy*, Vol. 40, No. 6, 743-748, doi:[10.3109/03639045.2013.782503](https://doi.org/10.3109/03639045.2013.782503)
- [4] Raichur, A.; Nakajima, Y.; Nagaoka, Y.; Maekawa, T.; Kumar, D. S. (2014). Hollow polymeric (PLGA) nano capsules synthesized using solvent emulsion evaporation method for enhanced drug encapsulation and release efficiency, *Materials Research Express*, Vol. 1, No. 4, paper 045407, doi:[10.1088/2053-1591/1/4/045407](https://doi.org/10.1088/2053-1591/1/4/045407)
- [5] Son, A. I.; Opfermann, J. D.; McCue, C.; Ziobro, J.; Abrahams III, J. H.; Jones, K.; Morton, P. D.; Ishii, S.; Oluigbo, C.; Krieger, A.; Liu, J. S.; Hashimoto-Torii, K.; Torii, M. (2017). An implantable micro-caged device for direct local delivery of agents, *Scientific Reports*, Vol. 7, paper 17624, 16 pages, doi:[10.1038/s41598-017-17912-y](https://doi.org/10.1038/s41598-017-17912-y)
- [6] Gao, Y.; Chen, T.; Wang, X. (2011). Numerical modeling of a novel degradable drug delivery system with microholes, *Microsystem Technologies*, Vol. 17, No. 3, 387-394, doi:[10.1007/s00542-011-1266-2](https://doi.org/10.1007/s00542-011-1266-2)
- [7] Kovacic, M.; Brezocnik, M. (2018). Reduction of surface defects and optimization of continuous casting of 70MnVS4 steel, *International Journal of Simulation Modelling*, Vol. 17, No. 4, 667-676, doi:[10.2507/IJSIMM17\(4\)457](https://doi.org/10.2507/IJSIMM17(4)457)
- [8] Zhang, W.; Yu, Y. (2018). High-temperature rheological behavior and numerical simulation technology for 6061 aluminum alloy connecting rods, *Journal of Engineering Science and Technology Review*, Vol. 11, No. 6, 116-124, doi:[10.25103/jestr.116.15](https://doi.org/10.25103/jestr.116.15)
- [9] Kim, S.; Lee, W.; Kim, D. (2015). One-step distortion simulation of pulsed laser welding with multi-physics information, *International Journal of Simulation Modelling*, Vol. 14, No. 1, 85-97, doi:[10.2507/ijssimm14\(1\)8.291](https://doi.org/10.2507/ijssimm14(1)8.291)
- [10] Rowland, H. D.; King, W. P. (2004). Polymer deformation and filling modes during microembossing, *Journal of Micromechanics and Microengineering*, Vol. 14, No. 12, 1625-1632, doi:[10.1088/0960-1317/14/12/005](https://doi.org/10.1088/0960-1317/14/12/005)
- [11] Xie, L.; Ziegmann, G. (2009). Influence of processing parameters on micro injection molded weld line mechanical properties of polypropylene (PP), *Microsystem Technologies*, Vol. 15, No. 9, 1427-1435, doi:[10.1007/s00542-009-0904-4](https://doi.org/10.1007/s00542-009-0904-4)
- [12] Su, Q.; Zhang, N.; Gilchrist, M. D. (2016). The use of variotherm systems for microinjection molding, *Journal of Applied Polymer Science*, Vol. 133, No. 9, paper 42962, doi:[10.1002/app.42962](https://doi.org/10.1002/app.42962)
- [13] Okwuosa, T. C.; Pereira, B. C.; Arafat, B.; Cieszynska, M.; Isreb, A.; Alhnan, M. A. (2017). Fabricating a shell-core delayed release tablet using dual FDM 3D printing for patient-centred therapy, *Pharmaceutical Research*, Vol. 34, No. 2, 427-437, doi:[10.1007/s11095-016-2073-3](https://doi.org/10.1007/s11095-016-2073-3)
- [14] Valerga Puerta, A. P.; Batista Ponce, M.; Fernandez Vidal, S. R.; Girot Mata, F. (2018). Post-processing of PLA parts after additive manufacturing by FDM technology, *DYNA*, Vol. 93, No. 6, 625-629, doi:[10.6036/8859](https://doi.org/10.6036/8859)
- [15] Chidambaram, N.; Kirchner, R.; Altana, M.; Schiff, H. (2016). High fidelity 3D thermal nanoimprint with UV curable polydimethyl siloxane stamps, *Journal of Vacuum Science & Technology B*, Vol. 34, No. 6, paper 06K401, doi:[10.1116/1.4961250](https://doi.org/10.1116/1.4961250)
- [16] Kiew, C. M.; Lin, W.-J.; Teo, T. J.; Tan, J. L.; Lin, W.; Yang, G. (2009). Finite element analysis of PMMA pattern formation during hot embossing process, *2009 IEEE/ASME International Conference on Advanced Intelligent Mechatronics*, Singapore, 314-319

- [17] Hung, C.; Chen, R.-H.; Lin, C.-R. (2002). The characterisation and finite-element analysis of a polymer under hot pressing, *The International Journal of Advanced Manufacturing Technology*, Vol. 20, No. 3, 230-235, doi:[10.1007/s001700200146](https://doi.org/10.1007/s001700200146)
- [18] Hirai, Y.; Onishi, Y.; Tanabe, T.; Shibata, M.; Iwasaki, T.; Iriye, Y. (2008). Pressure and resist thickness dependency of resist time evolutions profiles in nanoimprint lithography, *Microelectronic Engineering*, Vol. 85, No. 5-6, 842-845, doi:[10.1016/j.mee.2007.12.084](https://doi.org/10.1016/j.mee.2007.12.084)
- [19] Kim, N. W.; Kim, K. W.; Sin, H.-C. (2008). Finite element analysis of low temperature thermal nanoimprint lithography using a viscoelastic model, *Microelectronic Engineering*, Vol. 85, No. 9, 1858-1865, doi:[10.1016/j.mee.2008.05.030](https://doi.org/10.1016/j.mee.2008.05.030)
- [20] Lan, S.; Lee, H.-J.; Lee, S.-H.; Ni, J.; Lai, X.; Lee, H.-W.; Song, J.-H.; Lee, M. G. (2009). Experimental and numerical study on the viscoelastic property of polycarbonate near glass transition temperature for micro thermal imprint process, *Materials & Design*, Vol. 30, No. 9, 3879-3884, doi:[10.1016/j.matdes.2009.03.045](https://doi.org/10.1016/j.matdes.2009.03.045)
- [21] Fu, G.; Loh, N. H.; Tor, S. B.; Tay, B. Y.; Murakoshi, Y.; Maeda, R. (2006). Analysis of demolding in micro metal injection molding, *Microsystem Technologies*, Vol. 12, No. 6, 554-564, doi:[10.1007/s00542-005-0071-1](https://doi.org/10.1007/s00542-005-0071-1)
- [22] Hirai, Y., Fujiwara, M.; Okuno, T.; Tanaka, Y.; Endo, M.; Irie, S.; Nakagawa, K.; Sasago, M. (2001). Study of the resist deformation in nanoimprint lithography, *Journal of Vacuum Science & Technology B*, Vol. 19, No. 6, 2811-2815, doi:[10.1116/1.1415510](https://doi.org/10.1116/1.1415510)
- [23] Chen, C.; Chen, T.; Wang, X. (2012). Stress relaxation properties of biodegradable polymer PLGA, *Polymer Materials Science & Engineering*, Vol. 28, No. 1, 60-62, doi:[10.16865/j.cnki.1000-7555.2012.01.017](https://doi.org/10.16865/j.cnki.1000-7555.2012.01.017)
- [24] Gokce, H. (2018). Prediction of nonlinear dynamic impact force history by finite element method, *Journal of Engineering Science and Technology Review*, Vol. 11, No. 3, 50-55, doi:[10.25103/jestr.113.07](https://doi.org/10.25103/jestr.113.07)